PROCEEDINGS OF SCIENCE

Search for dark matter annihilations in the Sun using the completed IceCube neutrino telescope.

The IceCube Collaboration[†],

[†] *http://icecube.wisc.edu/collaboration/authors/icrc15_icecube*

E-mail: Mohamed.Rameez@cern.ch

Dark matter particles after scattering off nuclei would be gravitationally captured in the Sun where they may pair-annihilate into standard model particles. Terrestrial neutrino detectors such as IceCube can observe this as an enhanced neutrino flux from the direction of the Sun. We present results from an analysis of 341 days of livetime of IceCube-DeepCore in the 86 string configuration. The sensitivity has improved with respect to previous searches due to better analysis methods and reconstructions. In addition, improved veto techniques using the outer layers of the cubic kilometre array have been used to reduce the atmospheric muon background and thus enhance sensitivity during the austral summer.

Corresponding authors: M. Rameez[*1], T. Montaruli[1], S. Vallecorsa[1],

[1] *Département de physique nucléaire et corpusculaire, Université de Genève, 24 Quai Ernest Ansermet, 1211 Genève, Switzerland*

The 34th International Cosmic Ray Conference,
30 July- 6 August, 2015
The Hague, The Netherlands

[*] Speaker.

PoS(ICRC2015)1209

1. Introduction

Astrophysical observations provide strong evidence for the existence of dark matter(DM). However the nature of DM is unknown. An interesting and experimentally accessible candidate is the so called 'Weakly Interacting Massive Particle (WIMP)'(see [1] for a comprehensive review) - expected to exist in the mass range of a few GeVs to a few TeVs. If DM consists of WIMPs, they will be gravitationally captured by the Sun [2], where they may pair-annihilate into standard model particles, including neutrinos. Given enough time, the capture and annihilation processes would reach equilibrium [3] and on average only as many WIMPs annihilate as are captured per unit time. This DM-generated neutrino flux may be detected at terrestrial neutrino detectors such as IceCube. As the region at the centre of the Sun where most of the annihilations will occur is very small, the search is equivalent to looking for a point-like source of neutrinos. However, neutrinos above 1 TeV have interaction lengths significantly smaller than the radius of the Sun and are mostly absorbed. As a result all the signal is expected in the range of a few GeVs to $\sim$1 TeV, making this a very low energy point-source search for IceCube. The energies are nevertheless high enough that such neutrinos can never be made by nuclear fusion processes in the Sun.

2. The Detector

IceCube is a cubic-kilometer neutrino detector installed in the ice at the geographic South Pole [8] between depths of 1450 m and 2450 m. Detector construction started in 2005 and finished in 2010. Neutrino reconstruction relies on the optical detection of Cherenkov radiation emitted by secondary particles produced in neutrino interactions in the surrounding ice or the nearby bedrock. At the center of the array, there are 8 more densely instrumented strings containing Digital Optical Modules (DOMs) with higher quantum efficiency photomultiplier tubes, optimized for lower energies. Along with 7 adjacent standard strings, these are defined as the DeepCore sub-array for the purpose of this analysis.

3. Event Selection

Neutrino flux predictions at Earth from WIMP annihilations in the Sun have been widely studied, for example in Ref [4]. We use the flux predictions from DarkSuSy [5] and WimpSim [4] to simulate signals for the IceCube detector according to specific annihilation scenarios. The energy range of the expected signal (a few TeV at maximum) and the properties of IceCube at these energies dictate the event selection strategies. While the principal IceCube array has an energy threshold of $\sim$100 GeV, the more densely instrumented DeepCore infill array has an energy threshold of $\sim$10 GeV. This means that for WIMP masses < 200 GeV, which produce signal neutrinos mostly with energies below the IceCube threshold, only DeepCore[6] will contribute significantly towards the effective volume. However, for higher WIMP masses where a significant fraction of the resultant neutrinos are above the IceCube threshold, the full effective volume of IceCube comes into play. For optimizing the event selections for the analysis and setting upper limits, we consider two scenarios: WIMPs annihilating completely into W^+W^-, a 'hard' channel with emission peaked at neutrino energies close to the WIMP mass, and WIMPs annihilating completely into $b\bar{b}$, a 'soft'

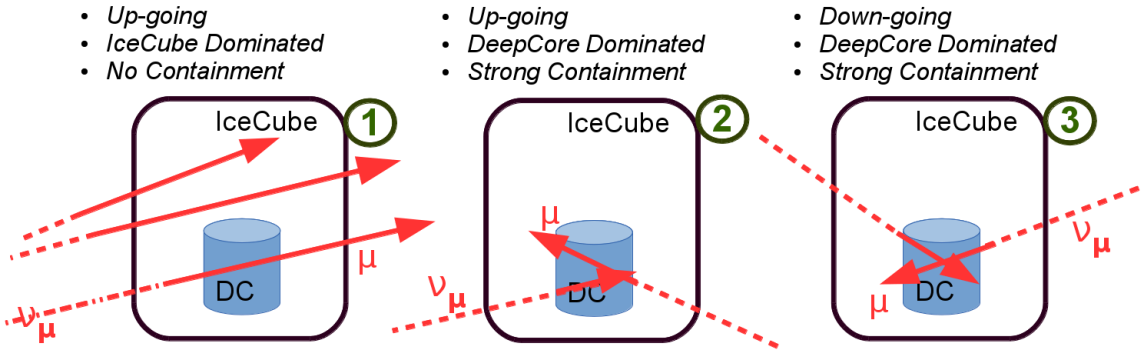

Figure 1: The three event selection strategies for the solar WIMP analysis. Most of the sensitivity for neutrino signals below 100 GeV comes from the DeepCore (DC) dominated low energy samples(2 and 3). During the austral summer (when the Sun is a source of downgoing neutrinos), the very large muon background forces us to use the outer detector as a Veto (see Fig. 2) and consequently there is only a DeepCore dominated-low energy sample (3). This approach is similar to that of earlier IceCube analyses such as [7].

channel with emission peaked at neutrino energies of a few GeV. Since IceCube acceptance is very energy dependent, cuts have to be optimized for the spectral composition of the expected signal flux. For WIMP masses below 80.4 GeV, we also consider a WIMP annihilating into $\tau\bar{\tau}$, since annihilations to W^+W^- are no longer kinematically allowed.

Within IceCube, a standard set of filters are used to pre-select signal-like muon events and reduce the rate of the dominant atmospheric background. This analysis starts with a stream of data from three of these filters, a low-energy DeepCore filter and two filters selecting muon-like events that point upwards; one favouring short low energy tracks and another that favours bright through-going tracks. After these filters the data rate is ~ 100 Hz. From this point onwards, data are treated differently depending upon whether they fall in the austral winter or summer.

During the austral winter, when the Sun is below the horizon, the signal consists of upgoing neutrinos. The background is dominantly made up of downgoing atmospheric muons falsely reconstructed as upgoing. Reconstructed event properties quantifying topology, track length, reconstruction quality etc are used to reject background such as very high energy events or vertical events which obviously cannot come from the Sun and reduce the data to ~ 2 Hz. At this point, a likelihood reconstruction with a prior based on the zenith distribution, which takes into account that the majority of the tracks are downgoing atmospheric muons, is performed to identify and remove falsely reconstructed downgoing events. Depending upon the location of the majority of detected Cherenkov photons (whether within IceCube (1) or within DeepCore (2)), events are split into two streams (see Fig 1). Subsequently, separate instances of a multivariate classification algorithm, known as Boosted Decision Tree (BDT), are used to select signal-like events from both these streams. The BDT of the IceCube dominated sample (1) is optimized for events from a 1 TeV WIMP annihilating into the hard W^+W^- channel while the DeepCore dominated sample (2) is optimized for events from 100 GeV and 50 GeV WIMPs annihilating into W^+W^-, $b\bar{b}$ and $\tau^+\tau^-$ channels. After the selection based on the BDT classifier, event rates of the two samples are ~ 2.9 mHz and ~ 0.34 mHz, respectively, consistent with expectations from a background that is dominated by atmospheric neutrinos.

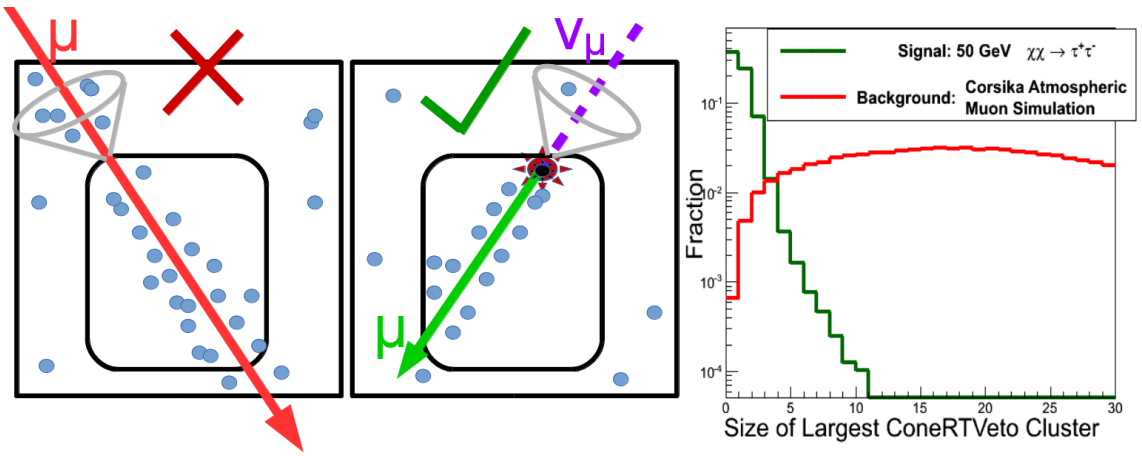

Figure 2: On the left and center: A schematic representation of the veto concept to reject atmospheric muon background and retain neutrinos during austral summer. Only events with their reconstructed vertex near DeepCore are selected. Subsequently, the photon detections within a cone of 40° half-angle at the vertex and aligned along the muon track are sorted into clusters based on whether they are within a specific 'Radius + Time (RT)' radius of each other. The size of the largest of these clusters of hits is reported. On the right: size of this cluster for signal (green) and background (red). Selecting events with cluster sizes ≤ 3 will keep more than 90% of signal while rejecting more than 90% of background of atmospheric muons.

During the austral summer (23rd September 2011 to 16th March 2012), the signal (downgoing) is overwhelmed by a background of downgoing atmospheric muons ($\sim 10^6$ times higher in rate) in addition to the atmospheric neutrinos. A sample of DeepCore dominated downgoing tracks ((3) in Fig 1) can be isolated by using the outer laters of IceCube as a veto (see Fig. 2). This sample is again optimized using a BDT algorithm to select events expected from 100 GeV and 50 GeV WIMPs annihilating into W^+W^-, $b\bar{b}$ and $\tau^+\tau^-$ channels. After the BDT-based event selection the even rate is ~ 0.24 mHz, consistent with the expected residual atmospheric neutrino and muon background.

Fig. 3 summarizes final effective areas and angular resolutions of the three samples.

4. Analysis method

The significance of a cluster of events in the direction of the Sun can be estimated using a modified version of the unbinned maximum likelihood ratio method described in Ref. [9]. Due to the very large point spread function of IceCube at these low neutrino energies, we model the spatial signal p.d.f of Ref. [9] as a Fisher-Bingham distribution from directional statistics [10].

For the fully contained events of the DeepCore dominated samples ((2) and (3) of Figure 1), the energy of the neutrino can be estimated by summing the energy of the muon (obtained by reconstructing the starting and stopping vertex of the muon) and the hadronic cascade from the charged current interaction. Signal and background p.d.f.s are constructed from the signal simulation and datasets randomized in azimuth respectively. Energy weighting is added to the likelihood to enhance sensitivity. Thus the signal p.d.f. is given by:

$$S_i(|\vec{x}_i - \vec{x}_{sun}(t_i)|, E_i, m_\chi, c_{ann}) = \mathscr{K}(|\vec{x}_i - \vec{x}_{sun}(t_i)|, \kappa_i) \times \mathscr{E}_{m_\chi, c_{ann}}(E_i), \tag{4.1}$$

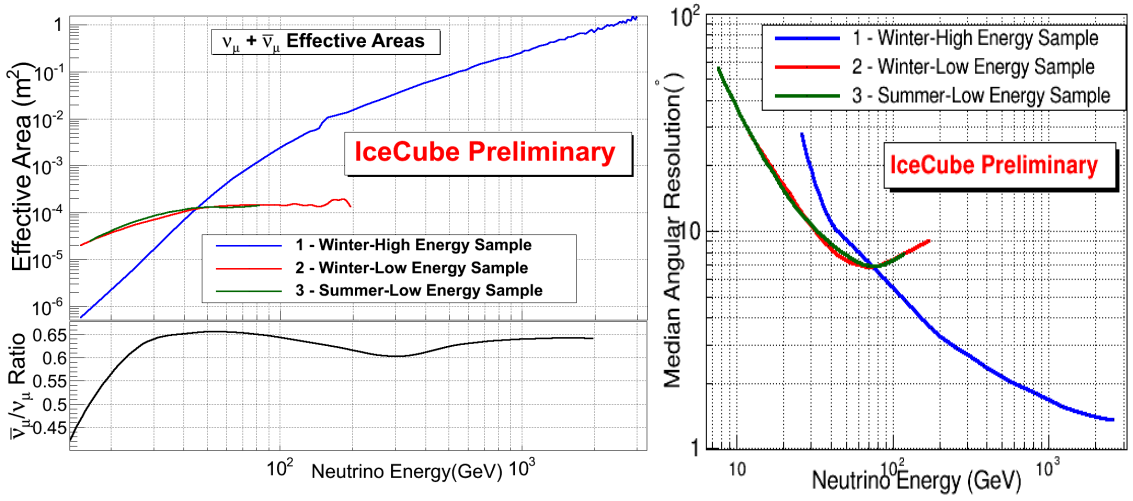

Figure 3: Top Left: $\nu_\mu + \bar{\nu}_\mu$ effective areas for the three different event selections. Bottom Left : Ratio of the $\bar{\nu}_\mu$ and ν_μ effective areas, determined by the relative cross sections and inelasticities of $\bar{\nu}_\mu$ and ν_μ. Right: The angular resolutions of the three samples at different energies, defined as the median of the angular separation between the incoming neutrino and the reconstructed muon.

where $\mathscr{K}$ stands for the spatial and $\mathscr{E}$ for the spectral parts of the p.d.f. and m_χ and c_{ann} stand for the mass and annihilation channel of the WIMP respectively.

$$\mathscr{K}(|\vec{x}_i - \vec{x}_{sun}(t_i)|, \kappa_i) = \frac{\kappa_i e^{\kappa_i cos(\theta_{|\vec{x}_i - \vec{x}_{sun}(t_i)|})}}{2\pi(e^{\kappa_i} - e^{-\kappa_i})} \tag{4.2}$$

where the concentration factor κ_i of the monovariate Fisher-Bingham distribution is obtained from the likelihood based estimate of the angular resolution of the track reconstruction [11].

The backgroung p.d.f. is:

$$\mathscr{B}_i(\vec{x}_i, E_i) = B(\delta_i) \times P(E_i|\phi_{atm}) \tag{4.3}$$

where $B(\delta_i)$ is the declination dependence and $P(E|\phi_{atm})$ indicates the distribution of the energy estimater E of the data sample at analysis level which is consistent with expectations from atmospheric muon and neutrino fluxes and is denoted by ϕ_{atm}.

The spatial p.d.f of the signal and the energy p.d.f of a specific signal and background are illustrated in Fig. 4.

For a sample of N events consisting of n_s signal events from the Sun and $N - n_s$ background events, the likelihood can then be written as:

$$\mathscr{L}(n_s) = \prod_N \left(\frac{n_s}{N} S_i + (1 - \frac{n_s}{N})\mathscr{B}_i\right) \tag{4.4}$$

The best estimate for the number of signal events in the sample is obtained by maximizing the likelihood ratio as defined in Ref. [9]. The significance of the observation can be estimated without depending on Monte Carlo simulations by repeating the process on datasets scrambled in right ascension. As the three separate event selections have no events in common, they can be combined

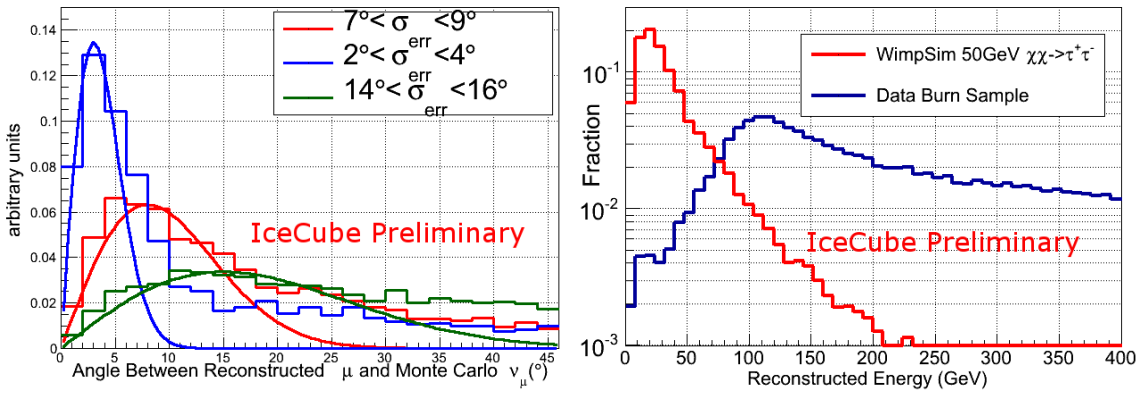

Figure 4: Left: Distribution of the angle between the Monte Carlo neutrino and the reconstructed muon for Monte Carlo events in three different ranges of angular resolutions of the track reconstruction. The histograms denote the observed distribution from Monte Carlo while the smooth curves are the analytical predictions from the Fisher Bingham distribution. While a better description of the tails can improve the sensitivity of this search, the impact will be small due to the small fraction of events present. Right: Normalized distributions of the reconstructed energy observed in real data as well as in signal Monte Carlo for 50 GeV WIMPs annihilating into the $\tau^+\tau^-$ channel. Both plots are for the Winter Low Energy selection.

statistically using the method described in [12]. Confidence intervals on the number of signal events present within the sample are constructed using the method of Feldman and Cousins[13].

5. Results and discussion

No significant excess was found in the direction of the Sun, allowing us to set stringent limits on the neutrino flux from the Sun in the GeV-TeV range. Assuming a local DM density of 0.3 GeV/cm^3, a standard Maxwellian halo velocity distribution and the Standard Solar Model, this limit can also be interpreted as a limit on the WIMP-nucleon scattering cross section. For the spin dependent case, IceCube limits are the most competitive in the region above $\sim$ 150 GeV (Fig. 5). Limits have improved by a factor of $\sim$30% to 60% w.r.t. the previous IceCube analysis [7]. The uncertainties on these limits due to uncertainties in velocity distributions of DM have been quantified in [20] and turn out not to be not greater than $\sim$ 50%. The study also concludes that these limits are conservative with regard to the possible existence of a dark-disk. A second independent solar wimp analysis carried out on the same data set has achieved a consistent level of sensitivity and is presented as separate contribution to ICRC[14].

Two more years of IceCube data are being analyzed using a similar approach and sensitivities are expected to improve further.

In specific supersymmetric models such as the MSSM [21] where the lightest stable state is the neutralino - a good WIMP candidate, these results can be used to constrain the parameter space of such models. More generally, the limits can be interpreted as limits on coupling strengths and mediator masses in certain Effective Field Theories(EFTs), parameter space of which can also be explored at collider searches [23, 24].

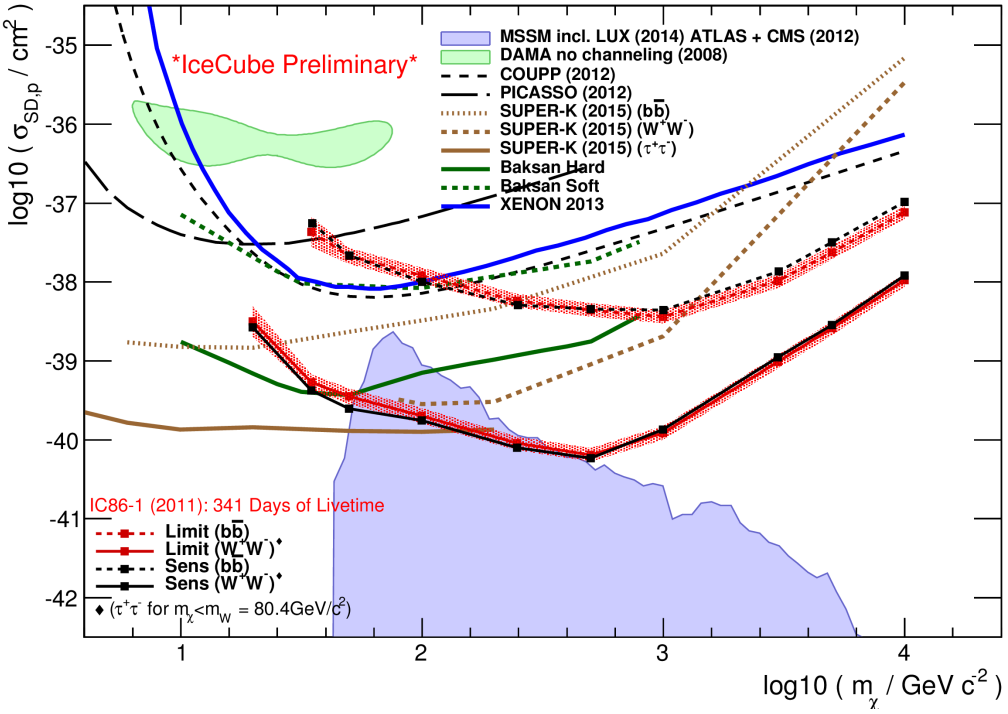

Figure 5: Limits on the spin dependent WIMP-Nucleon scattering cross section as a function of the WIMP mass, derived from this analysis and compared to other experiments' limits from [15, 18, 19, 21, 22]. The red band around the limit signifies systematic uncertainties.

References

[1] G. Bertone *et al*, Phys Rep., **405** (2005) p.279

[2] A. Gould *et al*, 1987 ApJ, vol. **321**, Oct. 1, 1987, p. 571-585.

[3] G. Jungman *et al*, Phys.Rept. **267** (1996) 195-373

[4] M. Blennow, J. Edsjö and T. Ohlsson, JCAP **01**, 021 (2008)

[5] P. Gondolo, J. Edsjö, P. Ullio, L. Bergström, M. Schelke and E.A. Baltz, JCAP **07**, 008 (2004)

[6] R. Abbasi *et al.*, [IceCube Coll.], Astropart. Phys. **35** (2012).

[7] M. G. Aartsen *et al.* [IceCube Coll.], Phys. Rev. Lett. **110**, 131302 (2013)

[8] A. Achterberg *et al.* [IceCube Coll.], Astropart. Phys. **26** 155. (2006)

[9] J. Braun *et al*, Astropart.Phys. **29**, 299-305 (2008).

[10] J.T. Kent, J. Royal. Stat. Soc., **44** 71-80 (1982)

[11] T. Neunhoffer, Astropart.Phys. **25**, 220-225 (2006).

[12] M. G. Aartsen *et al.* [IceCube Coll.], ApJ **796** (2014) 109.

[13] G. Feldman and J. Cousins, Phys.Rev.D **57** 3873-3889 (1998)

[14] IceCube Coll., PoS (ICRC2015) 1099 these proceedings

[15] M. M. Boliev *et al.* JCAP **09**, 019 (2013)

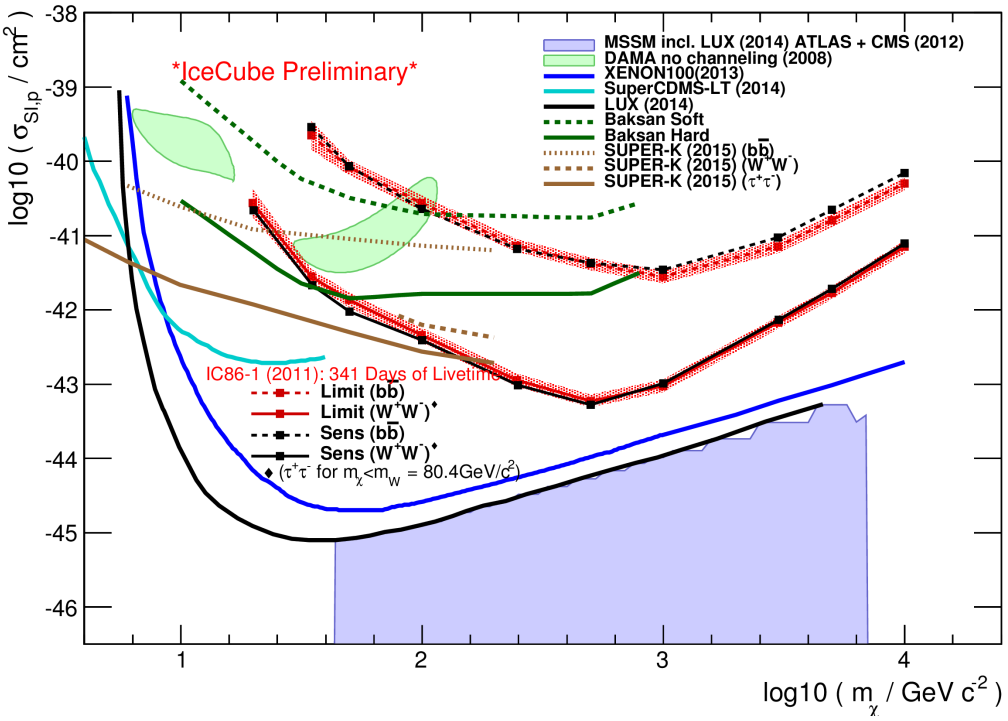

Figure 6: Similar limits on the spin independent WIMP-Nucleon scattering cross section compared to limits from [15, 16, 17, 18, 22]

[16] D. S. Akerib *et al.* [LUX Coll.], Phys. Rev. Lett. **112**, 091303 (2013).

[17] R. Agnese *et al.* [SuperCDMS Coll.], Phys. Rev. Lett. **112**, 241302 (2014).

[18] E. Aprile *et al.* [XENON Coll.], Phys. Rev. Lett, **109**, 181301 (2012).

[19] R. Bernabei *et al.*, Eur. Phys. J. C. **53** (2008), 205.

[20] K. Choi *et al.*, JCAP **05**, 049 (2014)

[21] H. Silverwood *et al.*, JCAP **03**, 027 (2013)

[22] K. Choi *et al.* [Super-Kamiokande Coll.], Phys. Rev. Lett. **114**, 141301 (2015)

[23] J. Blumenthal *et al.*, Phys. Rev. D **91**, 035002, 2015

[24] R. Catena, JCAP **04**, 052 (2015)